Acidic sphingomyelinase downregulates the liver-specific methionine adenosyltransferase 1A, contributing to tumor necrosis factor–induced lethal hepatitis

Montserrat Marí,[1] Anna Colell,[1] Albert Morales,[1] Covadonga Pañeda,[2] Isabel Varela-Nieto,[2] Carmen García-Ruiz,[1,3] and José C. Fernández-Checa[1,3]

[1]Liver Unit, Institut de Malalties Digestives, Hospital Clínic i Provincial, Instituto Investigaciones Biomédicas August Pi i Sunyer, Barcelona, Spain. [2]Instituto Investigaciones Biomédicas Alberto Sols, Consejo Superior Investigaciones Científicas, Madrid, Spain. [3]Department of Experimental Pathology, Instituto Investigaciones Biomédicas Barcelona, Consejo Superior de Investigaciones Científicas, Barcelona, Spain.

_S_-adenosyl-L-methionine (SAM) is synthesized by methionine adenosyltransferases (MATs). Ablation of the liver-specific *MAT1A* gene results in liver neoplasia and sensitivity to oxidant injury. Here we show that acidic sphingomyelinase (ASMase) mediates the downregulation of MAT1A by TNF-α. The levels of MAT1A mRNA as well as MAT I/III protein decreased in cultured rat hepatocytes by in situ generation of ceramide from exogenous human placenta ASMase. Hepatocytes lacking the *ASMase* gene (*ASMase*$^{-/-}$) were insensitive to TNF-α but were responsive to exogenous ASMase-induced downregulation of MAT1A. In an in vivo model of lethal hepatitis by TNF-α, depletion of SAM preceded activation of caspases 8 and 3, massive liver damage, and death of the mice. In contrast, minimal hepatic SAM depletion, caspase activation, and liver damage were seen in *ASMase*$^{-/-}$ mice. Moreover, therapeutic treatment with SAM abrogated caspase activation and liver injury, thus rescuing *ASMase*$^{+/+}$ mice from TNF-α–induced lethality. Thus, we have demonstrated a new role for ASMase in TNF-α–induced liver failure through downregulation of MAT1A, and maintenance of SAM may be useful in the treatment of acute and chronic liver diseases.

Introduction

TNF-α plays a central role in many forms of liver injury (1–3) and hence information on signaling of hepatocellular cell death by TNF-α may be of therapeutic relevance. The signaling mechanism mediating the intracellular effects of TNF-α is complex and can lead to multiple responses, including proliferation, inflammation, or cell death. The cytotoxic effects of TNF-α are the result of the generation of death signals that originate from the binding of TNF-α to the TNF-α–R1 receptor, a typical death receptor with a 60– to 80–amino acid cytoplasmic sequence known as the death domain. Research in this area has unveiled complex protein-protein interactions, recruitment of signaling intermediates, and activation of proteins that mediate the apoptotic effect of TNF-α (4, 5). Ceramide has emerged as a putative signaling lipid mediator that plays a role in the stress response, cell death, and TNF-α signaling (6–9). Ceramide levels can increase by de novo synthesis through activation of serine-palmitoyl transferase, the rate-limiting enzyme in ceramide synthesis, or ceramide synthetase (10, 11). However, the hydrolysis of sphingomyelin upon activation of sphingomyelinases (SMases) constitutes an effective means for the rapid generation of ceramide (8, 9). The binding of TNF-α to its plasma membrane receptor TNF-α–R1 results in the activation of two major types of SMases: a neutral SMase (NSMase), with an optimum pH around 7.5, which is membrane bound and Mg^{2+} dependent; and an acidic SMase (ASMase), with an optimum pH of about 4.8, which is further subclassified into two isoforms, an endosomal/lysosomal ASMase and a secretory Zn^{2+}-dependent ASMase (8, 9, 12, 13).

While activation of these enzymes may generate ceramide at different cellular sites that mediate the diverse effects of TNF-α, their role in apoptosis is not well established. Thus, NSMase has been reported to be involved in the stress response mediating the cytotoxic effects exerted by chemotherapeutic agents (14), whereas ASMase has been shown to play an essential role in ionizing radiation–mediated cell death (15, 16) as well as in the developmental death of oocytes (17). In addition, the factor associated with NSMase activation, an adaptor protein involved in NSMase activation, has been shown to contribute to TNF-α–induced fibroblast apoptosis (18), although the role of NSMase ablation itself in TNF-α–induced apoptosis remains unknown. On the other hand, the role of ASMase in Fas-induced cell death appears to be restricted to hepatocytes, as the absence of ASMase in hepatocytes has been shown to confer resistance to Fas-mediated cell death (19, 20), while other cell types from ASMase knockout mice are sensitive to Fas (19). Moreover, we have recently demonstrated that ASMase plays a significant role in hepatocellular apoptosis and liver damage induced by TNF-α (21).

The liver plays a prominent role in the synthesis and consumption of _S_-adenosyl-L-methionine (SAM, also abbreviated as "AdoMet"), which functions as the one-carbon donor for methylation of DNA,

Nonstandard abbreviations used: acidic sphingomyelinase (ASMase); alanine aminotransferase (ALT); *Bacillus cereus* sphingomyelinase (bNSMase); D-(+)-galactosamine (Gal); D-*threo*-1-phenyl-2-decanoylamino-3-morpholino-propanol HCl (D-*threo*-PDMP); ganglioside GD3 (GD3); ganglioside GM3 (GM3); glucosylceramide synthase (GCS); γ-glutamylcysteine synthetase (γ-GCS); glutathione (GSH); human placenta sphingomyelinase (hASMase); L-buthionine sulfoximine (BSO); liver-specific methionine adenosyltransferase (MAT1A); mannose 6-phosphate (M 6-P); methionine adenosyltransferase (MAT); *N*-acetylcysteine (NAC); neutral sphingomyelinase (NSMase); *S*-adenosyl-L-homocysteine (SAH); *S*-adenosyl-L-methionine (SAM); sphingomyelinase (SMase).

Conflict of interest: The authors have declared that no conflict of interest exists.

Citation for this article: *J. Clin. Invest.* **113**:895–904 (2004). doi:10.1172/JCI200419852.

RNA, and proteins and in the synthesis of biogenic amines and glutathione (GSH) (22–24). Furthermore, SAM is also required for DNA and RNA methylation in mitochondria and as an intermediate in the biosynthesis of ubiquinone and for sterol methylation (25, 26). SAM is synthesized from methionine and ATP by methionine adenosyltransferases (MATs). In mammals there are three known MAT isoforms (MAT I, MAT II, and MAT III) (23, 27, 28); MAT I and MAT III are a tetramer and a dimmer, respectively, of the same α1 subunit, a 43.7-kDa polypeptide encoded by the gene *MAT1A*, which is exclusively expressed in adult liver (23). MAT2A, on the other hand, is ubiquitously expressed and encodes a catalytic subunit (α2) found in a native MAT isoenzyme (MAT II) in association with a regulatory β subunit (29). In the liver, impairment of MAT I/III results in lowered SAM levels, which contributes to the progression of liver injury in experimental models and in patients with alcohol- or virus-induced cirrhosis (23, 30–33). Indeed, the most compelling evidence for the relevance of hepatic SAM has been recently documented with the development of *MAT1A* knockout mice (34). This paradigm illustrates the devastating consequences of chronic hepatocellular SAM depletion, which enhances the susceptibility of the liver to oxidant-induced cell death, metabolic disturbances, and spontaneous hepatocellular carcinoma (34, 35).

A common strategy for investigating the cellular effects of ceramide has been the incubation of cells with exogenous SMases, cell-permeable analogs, or natural ceramide, which has revealed a wide spectrum of responses ranging from cell cycle arrest to proliferation, oxidative stress, apoptosis, and gene regulation (6, 8, 21, 36, 37). As for the effect on gene regulation, membrane-permeant ceramide analogs (C2 and C6) as well as exogenous NSMase have been shown to modulate the expression of specific genes such as cytochrome P450 2C11, α_1-acid glycoprotein, or γ-glutamylcysteine synthetase (γ-GCS) in rat hepatocytes, mimicking the effects of interleukin-1 or TNF-α (36, 37). In addition, we have recently reported that the cell-permeable ceramide C2 downregulated MAT1A expression in H35 rat hepatoma cells (38). Thus, the present study was undertaken to examine the regulation of MAT1A by individual SMases, namely *Bacillus cereus* NSMase (bNSMase) and human placenta ASMase (hASMase), previously characterized in rat hepatocytes (37), with the ultimate goal of assessing the contribution of ASMase to the regulation of MAT1A expression and to test the therapeutic role of SAM in TNF-α–induced fulminant liver failure.

Methods

Hepatocyte isolation and incubation with SMases and glycosphingolipids. ASMase knockout mice (C57BL/6 strain) were propagated using heterozygous breeding pairs (a generous gift from R. Kolesnick, Laboratory of Signal Transduction, Memorial Sloan-Kettering Cancer Center, New York, New York, USA; and E. Gulbins, University of Duisburg-Essen, Essen, Germany) and were genotyped as described previously (21). Hepatocytes from male Sprague-Dawley rats (200–300 grams) or male mice (8–12 weeks old) were isolated by collagenase perfusion with flow rates of 16–18 ml/min and 7–9 ml/min, respectively, and were cultured at a density of 2×10^6 cells on 60-mm dishes coated with rat tail collagen. Rat or mouse hepatocytes were incubated with recombinant human TNF-α (15–280 ng/ml; Preprotech EC, London, United Kingdom) or exogenous SMases (Sigma-Aldrich, St. Louis, Missouri, USA) by dilution of concentrated hASMase (250 U/0.55 ml in 50% glycerol, 25 mM potassium phosphate, pH 4.5, 0.1% Triton X-100, and 0.05 mM PMSF) and bNSMase (100 U/ml in 50% glycerol and 50 mM Tris-HCl, pH 7.5) with culture medium to a concentration of 0.1–1.0 U/ml as described previously (37). Some cultures were pretreated with D-*threo*-1-phenyl-2-decanoylamino-3-morpholino-propanol HCl (D-*threo*-PDMP), *N*-butyldeoxynojirimycin, bafilomycin A1, chloroquine, or mannose 6-phosphate (M 6-P) before the addition of TNF-α or hASMase. Alternatively, cells were incubated with cell-permeable ceramide (C2 or C6), ganglioside GD3 (GD3), ganglioside GM3 (GM3), glucosylceramide, lactosylceramide, or lyso-glucosylceramide (1–5 μM) (Matreya, Pleasant Gap, Pennsylvania, USA) in ethanol (0.1%). In addition, cells were incubated with the natural ceramide C16 in dodecane/ethanol (2:98 [volume/volume]; 0.05% final concentration) or solvent only as a control. The experimental protocols met the guidelines of and were approved by the Animal Care Committee of the Hospital Clinic-Universidad de Barcelona.

Real-time PCR. MAT1A and MAT2A mRNA levels were determined by real-time RT-PCR analyses using a LightCycler and a Faststart SYBR Green I DNA quantification kit (Roche, Mannheim, Germany) following the manufacturer's protocol. cDNA was prepared from total RNA (2 μg) at 50°C for 50 minutes using random hexamers and the SuperScript III First-Strand Synthesis System for RT-PCR (Invitrogen, Carlsbad, California, USA) following the manufacturer's protocol. The primers used were: MAT1A, forward, 5′-ATGGACCTGTGGATGGC-3′, and reverse, 5′-TGGCCTCCAGTGTTATGT-3′; MAT2A, forward, 5′CCATGAGGCGTTCATCG-3′, and reverse, 5′-GCGTAACCAAGGCAATG-3′; 18S, forward, 5′-GGGGAATCAGGGTTCGATT-3′, and reverse, 5′-GCGCCGGTCCAAGAATTTCA-3′. The second-derivative maximum method was taken to determine the crossing points automatically for individual samples, and relative amounts of target genes were calculated based on the crossing-point analysis. The result was expressed as a ratio of product copies to copies of housekeeping gene *18S* from the same RNA.

Northern blot. MAT1A and MAT2A mRNA levels were also determined by Northern blot analyses of total RNA isolated using the Trizol reagent (Gibco/BRL, Grand Island, New York, USA). Ten micrograms of RNA were separated by electrophoresis under denaturing conditions and were transferred onto Hybond-XL nylon membranes (Amersham Biosciences, Uppsala, Sweden) and hybridized to random-primed ^{32}P-labeled cDNA probes.

MAT I/III protein levels. Samples were resolved by 12.5% SDS-PAGE, transferred to nitrocellulose membrane, and incubated with rabbit anti–MAT I/III (1:10,000 dilution), a generous gift from M. Pajares (Instituto Investigaciones Biomédicas Alberto Sols, Consejo Superior Investigaciones Científicas, Madrid, Spain), characterized previously (39). Membranes were incubated with peroxidase-conjugated secondary antibodies (1:5,000 dilution; Amersham, Arlington Heights, Illinois, USA), and bound antibody was visualized with ECL detection (ECL; Amersham) on Kodak X-OMAT film (Eastman Kodak, Rochester, New York, USA).

SAM/S-adenosyl-L-homocysteine (SAH), mitochondrial isolation, and GSH determination. SAM or SAH levels were determined in liver homogenates (or in mitochondrial fractions isolated from liver homogenates) after homogenization with 0.5 M $HClO_4$ followed by neutralization of the sample with 3 M KOH. SAM/SAH levels were determined by HPLC using a Partisil SCx 10-μm column by isocratic elution at a flow rate of 1 ml/min with 0.03 mol/l $NH_4H_2PO_4$ containing 2% acetonitrile, pH 2.6, as described before (33). SAM and SAH peaks were identified at 254 nm by sample spiking with authentic standards. The amount of either metabolite was calculated from standard curves relating the peak area to calibration curves with stan-

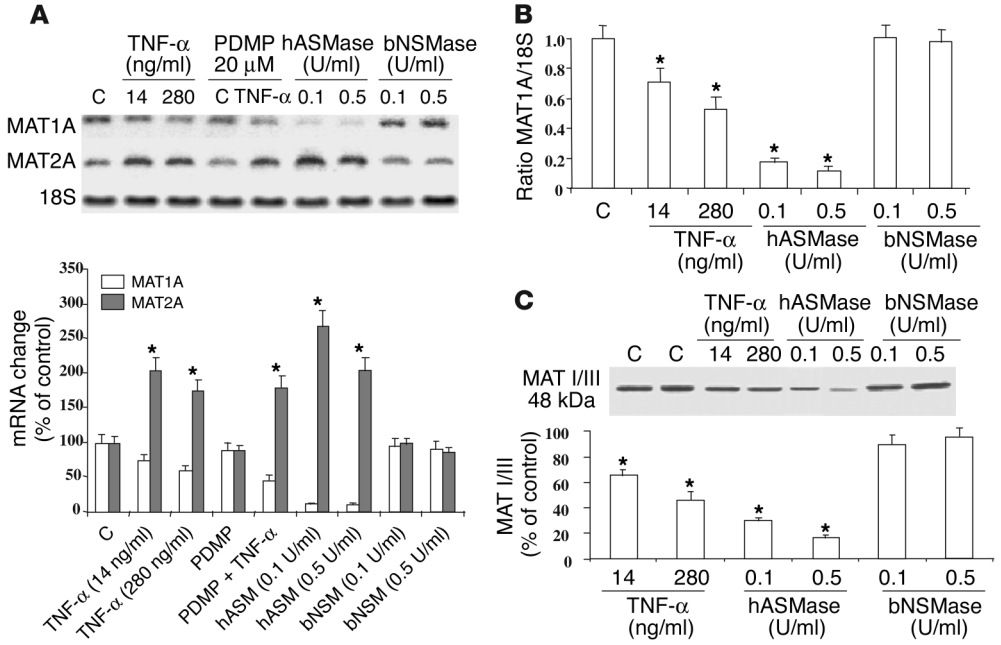

Figure 1
Regulation of MAT1A by SMases. (**A**) Cultured rat hepatocytes were treated with TNF-α, with or without D-*threo*-PDMP (PDMP), or with hASMase or bNSMase alone for 16 hours. MAT1A and MAT2A mRNA levels were analyzed by Northern blot and were normalized to 18S mRNA content, and the corresponding ratio was expressed as percentage of control. The plots in the graph (bottom) are the mean ± SD of six individual experiments. **P* < 0.05 versus control; denotes significance for MAT1A and MAT2A changes. (**B**) These experiments were similar to those shown in **A** except that MAT1A mRNA levels were determined by real-time PCR analyses as described in Methods. Results are expressed as the mean ± SD of three individual experiments. **P* = 0.05 versus control. (**C**) MAT I/III protein content was determined by Western blot after 18 hours of incubation with TNF-α, hASMase, or bNSMase at the dose shown. Data are the mean ± SD of three individual experiments. **P* = 0.05 versus control. C, control.

dards. In some cases, mitochondria were isolated by Percoll gradient centrifugation as described (40). GSH levels in homogenates or mitochondria were determined using HPLC (21, 37).

Fulminant hepatitis model and therapeutic treatment with SAM. The combination of D-(+)-galactosamine (Gal) plus TNF-α (Gal/TNF) or Gal plus LPS (Gal/LPS) is a known model of lethal hepatitis (41, 42). C57Bl/6 mice were used at an age of 8–10 weeks. A single dose of recombinant murine TNF-α (10 mg/kg intravenously; Preprotech EC, London, United Kingdom) or LPS (50 μg/kg intraperitoneally; *Escherichia coli* serotype 0128:B12; Sigma-Aldrich) was administered after Gal treatment (700 mg/kg intraperitoneally), resulting in the death of mice (90–95%) within 6–8 hours. In some cases, SAM (*p*-toluensulfonate form; Europharma, Madrid, Spain) was given hourly for 8 hours after TNF-α or LPS injection (5 mg/mouse intraperitoneally). For estimation of the effect of prolonged SAM treatment, SAM was administered to Gal/TNF- or Gal/LPS-treated mice for 24 hours (hourly for the first 8 hours and then every 8 hours). For blocking of GSH synthesis, L-buthionine sulfoximine (BSO) was administered (4 mmol/kg) 30 minutes before and 3 hours after TNF-α or LPS administration. Alternatively, *N*-acetylcysteine (NAC) (30 mg/mouse intraperitoneally) was given to mice before treatment with Gal/TNF or Gal/LPS to assess the efficacy of antioxidants on the course of liver injury. For histology, liver specimens were washed with PBS and embedded in paraffin. Sections 7 μm in thickness were stained with hematoxylin and eosin using standard methods. Serum alanine aminotransferase (ALT) and aspartate aminotransferase levels were determined by a colorimetric test (Sigma-Aldrich).

TUNEL assay. Paraffin-embedded liver tissue was cut into slices 4 μm in thickness using a microtome (Leica RM2155; Leica Instruments, Bensheim, Germany) and was fixed to glass slides. The TUNEL assay was performed by incubation of the slices with 2 μg/ml proteinase K (Sigma-Aldrich) in 10 mM Tris-HCl buffer containing 5 mM EDTA at a pH of 7.4. Sections were then labeled following the instructions of a commercial Kit (In situ Cell Death Detection Kit; Roche Diagnostics), stained with 3,3′-diaminobenzidine (Roche Diagnostics), and counterstained with hematoxylin and eosin. The slides were mounted and examined using a Nikon Eclipse E1000 microscope.

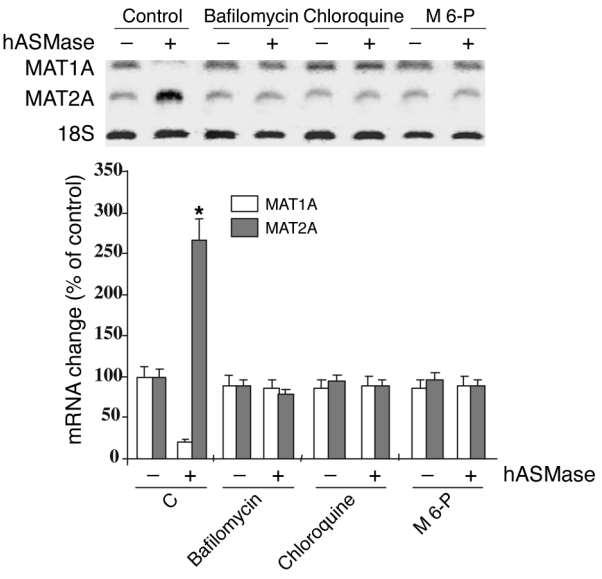

Figure 2
Regulation of the effect of hASMase on MAT1A expression. Cultured rat hepatocytes were incubated with hASMase (0.5 U/ml) for 16 hours in the presence of bafilomycin A1 (40 nM), chloroquine (50 μM), or M 6-P (3 mM), and the levels of MAT1A, MAT2A, and 18S mRNA were analyzed by Northern blot. The plot showing the change in the corresponding mRNA (bottom) is the mean ± SD of three individual experiments. **P* = 0.05 versus control; denotes significance for MAT1A and MAT2A changes.

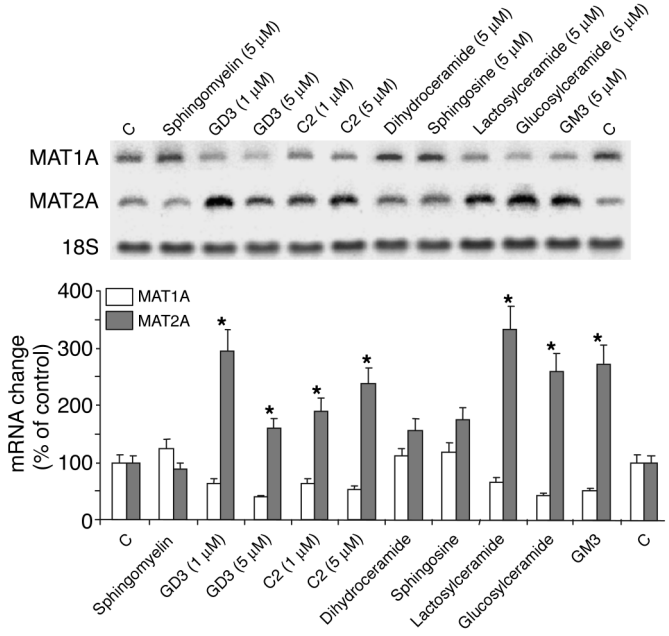

Figure 3
Regulation of MAT1A by sphingolipids. Cultured rat hepatocytes were incubated for 16 hours with various sphingolipids at the concentrations shown and the levels of MAT1A mRNA, MAT2A mRNA, and 18S mRNA were determined by Northern blot analyses. The plot showing the change in mRNA (bottom) is the mean ± SD of six individual experiments. *$P < 0.05$ versus control; denotes significance for MAT1A and MAT2A changes.

Caspase 3 and caspase 8 activation. Liver was homogenized in a buffer containing 120 mM NaCl, 50 mM Tris-HCl, pH 7.4, 0,5 % Igepal, 2 mM ethylene glycol-bis-(β-aminoethyl ether) tetraacetic acid, and 50 μM PMSF, incubated at 4°C for 15 minutes with shaking, and spun down at 12,000 *g* at 4°C for 15 minutes. Caspase activity was assayed with 200 μg of cell lysate and 1.25 ml of assay buffer containing 100 mM NaCl, 10% sucrose, 0.1% (3-[(3-cholamidopropyl)dimethylammonio]-1-propanesulfonate (CHAPS), and 10 mM DTT, pH 7.4, by the release of 7-aminomethyl coumarin from 40 nmol of Ac-DEVD-AMC (caspase 3) or Ac-IETD-AMC (caspase 8) (Calbiochem, San Diego, California, USA). Fluorescence was continuously recorded with emission at 460 nm and excitation at 380 nm as described (43).

In addition, caspase activation was also monitored by immunoblotting using rabbit anti–caspase 3 (1:1,000 dilution; Pharmingen, San Diego, California, USA) and anti–caspase 8 (1:100 dilution; Santa Cruz Biotechnology, Santa Cruz, California, USA) as primary antibodies. Membranes were then incubated with peroxidase-conjugated secondary antibodies (Amersham) and bound antibodies were visualized as described above for MAT I/III.

Measurement of gangliosides and ceramide levels. Gangliosides levels (including GM1, GM3, and GD3) were measured by high-performance thin-layer chromatography as described previously (43). Ceramide levels were quantified by HPLC (37).

TNF-α levels. Total TNF-α (bound and free) was measured in serum after Gal/LPS treatment using a mouse-specific competitive enzyme immunoassay kit (Chemicon, Temecula, California, USA).

Statistical analyses. Statistical analyses of mean values ± SD for multiple comparison were made by one-way analyses of variance followed by Fisher's exact test. Survival curves were compared using a log-rank χ^2 test.

Results

Regulation of MAT1A by hASMase. Preservation of high levels of MAT1A is critical for a differentiated and functional competent liver. Upon isolation from the intact organ, cultured rat hepatocytes undergo a gradual decline in MAT1A mRNA as it is replaced by MAT2A mRNA (23, 44). In vitro stabilization of MAT1A, however, can be achieved by the incubation of cultured hepatocytes with SAM (44). Because TNF-α downregulates MAT1A expression in cultured rat hepatocytes (38) and SMases mediate TNF-α signaling (8, 9), we first examined the role of individual SMases on MAT1A expression. Cultured rat hepatocytes were incubated with exogenous bNSMase and hASMase, and the levels of MAT1A and MAT2A mRNA were examined over time. Although the intracellular levels of ceramide generated by exposure of cultured hepatocytes to exogenous bNSMase or hASMase were equivalent (2–4 nmol ceramide/mg cellular protein), these enzymes regulated the expression of MAT1A and MAT2A in a divergent fashion. In the presence

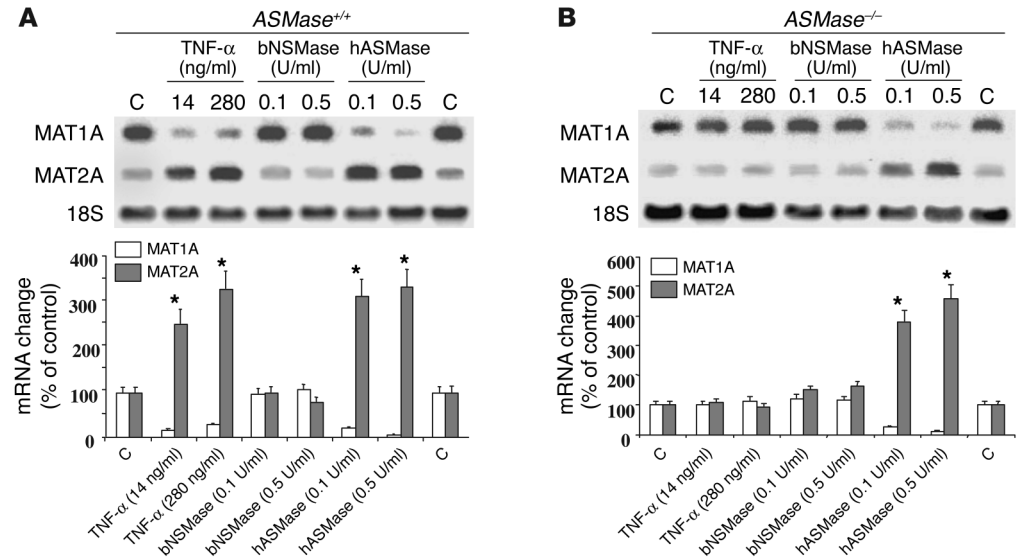

Figure 4
Regulation of MAT1A in hepatocytes from ASMase knockout mice. *ASMase*$^{+/+}$ (**A**) or *ASMase*$^{-/-}$ (**B**) hepatocytes were cultured for 16 hours with TNF-α, bNSMase, or hASMase at the dose shown, and the levels of MAT1A and MAT2A mRNA were determined by Northern blot. The plots (bottom) show the mean ± SD of six to seven individual experiments. *$P < 0.05$ versus control; denotes significance for MAT1A and MAT2A changes.

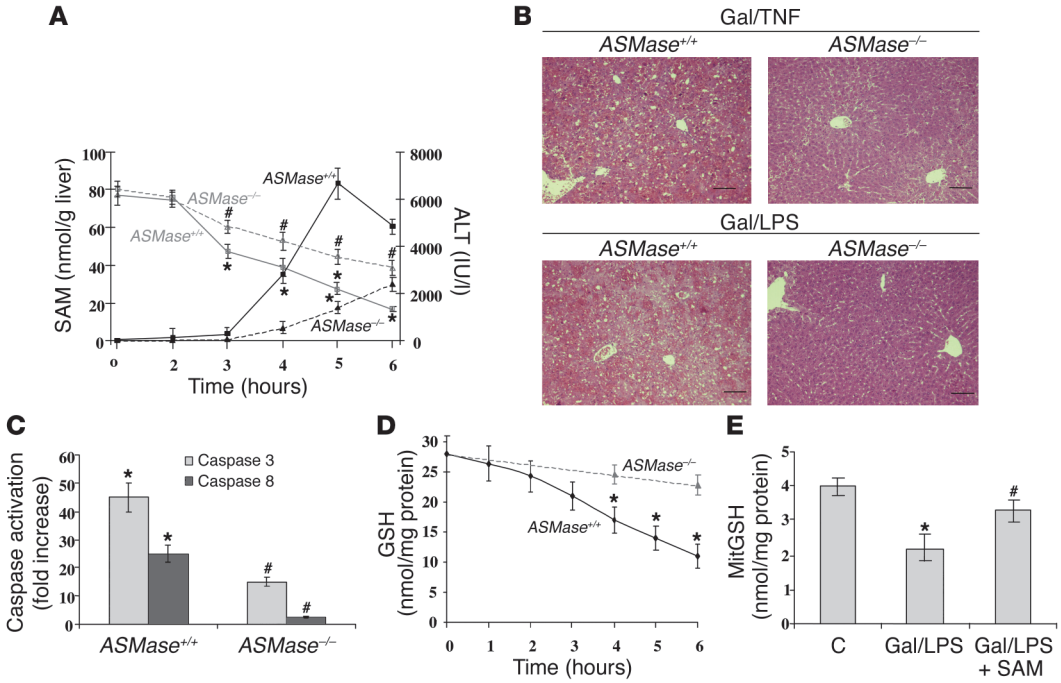

Figure 5

Fulminant hepatitis in *ASMase*$^{+/+}$ and *ASMase*$^{-/-}$ mice. (**A**) *ASMase*$^{+/+}$ and *ASMase*$^{-/-}$ mice (n = 25 each) were treated with Gal/TNF, and the levels of hepatic SAM were determined over time in relation to the appearance of liver damage, as monitored by serum ALT activity in serum. *P < 0.05 versus values at time 0; $^{\#}P$ < 0.05 versus corresponding time points from *ASMase*$^{+/+}$ mice. (**B**) Representative hematoxylin and eosin staining of liver sections from *ASMase*$^{+/+}$ or *ASMase*$^{-/-}$ mice collected 6 hours after treatment with Gal/TNF or Gal/LPS. Scale bars: 5 μm. (**C**) Caspase activity in liver samples taken from *ASMase*$^{+/+}$ or *ASMase*$^{-/-}$ 6 hours after treatment with Gal/TNF. *P < 0.05 versus control mice; $^{\#}P$ < 0.05 versus *ASMase*$^{+/+}$ mice. (**D**) Hepatic GSH levels were determined in liver samples from *ASMase*$^{+/+}$ and *ASMase*$^{-/-}$ mice at various times after treatment with Gal/TNF. *P < 0.05 versus values at time 0. (**E**) Mitochondrial fractions were prepared from the livers of *ASMase*$^{+/+}$ mice 6 hours after challenge with saline (C) or Gal/LPS with or without SAM administration given hourly as described in Methods. MitGSH, mitochondrial GSH. *P < 0.05 versus control; $^{\#}P$ < 0.05 versus Gal/LPS.

of exogenous SAM (3 mM), the level of MAT1A mRNA in control hepatocytes remained unchanged for 14–16 hours (not shown) in agreement with previous results (44). Next, we examined the effect of exogenous SMases on MAT1A mRNA by Northern blot and real-time PCR analyses. Either approach showed equivalent results, indicating a decrease in the levels of MAT1A mRNA by hASMase while those of MAT2A mRNA increased, thus mimicking the effect observed with TNF-α (Figure 1, A and B). In contrast, exogenous bNSMase did not affect the expression of MAT1A or MAT2A (Figure 1, A and B). The repressive effect of hASMase was observed within 3 hours of incubation, with a significant reduction in MAT1A mRNA levels to 39–45% of control values. To determine if the downregulation of MAT1A mRNA was reflected at the protein level, we analyzed the MAT I/III protein content by Western blot. As seen, both TNF-α and hASMase but not bNSMase reduced the levels of MAT I/III (Figure 1C). Consistent with these findings, we confirmed a severe reduction in MAT I/III enzymatic activity (8.7 ± 1.2 vs. 3.2 ± 0.8 pmol/min/mg protein in control or hASMase-treated cells, respectively; P < 0.05). Moreover, as TNF-α increases the cellular levels of glycosphingolipids synthesized in the Golgi from ceramide, and as glycosphingolipids play an important role in cell death (21, 43), we next examined the contribution of glycosphingolipids in the regulation of MAT1A by TNF-α. In agreement with previous results (21), preincubation of cells with D-*threo*-PDMP inhibited glucosylceramide synthase (GCS), the first enzyme in gly-

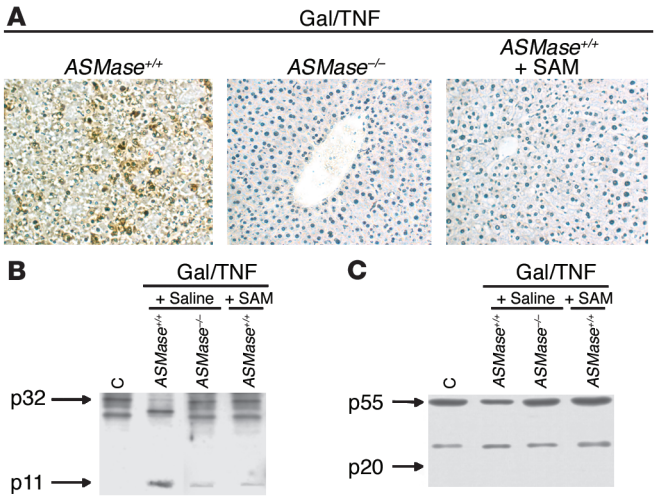

Figure 6

TUNEL assay and immunoblot analyses of caspase activation. (**A**) Liver samples from *ASMase*$^{+/+}$ or *ASMase*$^{-/-}$ mice treated with Gal/TNF or *ASMase*$^{+/+}$ mice treated with SAM for 8 hours were subjected to TUNEL assay for the detection of apoptotic hepatocytes (magnification, ×200). (**B** and **C**) Cellular extracts from these groups of mice were incubated with anti–caspase 3 (**B**) or anti–caspase 8 (**C**) to monitor the processing of the corresponding caspase. Representative immunoblots of three individual experiments showing similar results are shown.

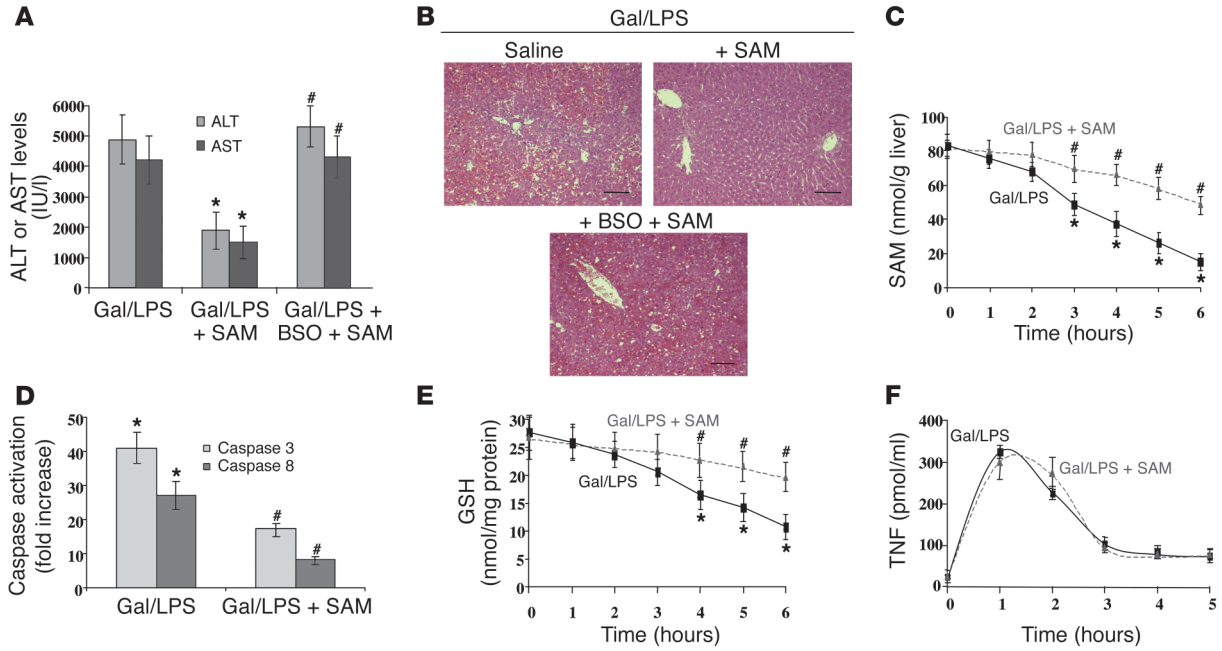

Figure 7

SAM therapy in fulminant hepatitis. Experimental *ASMase*$^{+/+}$ mice (n = 40) were treated with Gal/LPS; control mice (Saline, in **B**; n = 40) were treated with saline. Mice were divided in three groups: one group received SAM (5 mg/mouse intraperitoneally) or saline every hour for 8 hours after treatment with Gal/LPS; in addition, half of the mice receiving SAM therapy were pretreated with BSO (4 mmol/kg). (**A**) Serum ALT or AST levels. *P < 0.05 versus Gal/LPS; #P < 0.05 versus *ASMase*$^{+/+}$ mice treated with Gal/LPS + SAM. AST, aspartate aminotransferase. (**B**) Hematoxylin and eosin staining of livers with or without SAM administration or BSO treatment. Scale bars: 5 μm. (**C**) Hepatocellular SAM levels of *ASMase*$^{+/+}$ mice challenged with Gal/LPS with or without SAM therapy. *P < 0.05 versus values at time 0; #P < 0.05 versus Gal/LPS group. (**D**) Caspase activity in livers from *ASMase*$^{+/+}$ mice with or without SAM treatment. *P < 0.05 versus untreated mice; #P < 0.05 versus Gal/LPS group. (**E**) Hepatic GSH levels in *ASMase*$^{+/+}$ mice with or without SAM treatment. *P < 0.05 versus values at time 0; #P < 0.05 versus Gal/LPS group. (**F**) Serum TNF-α levels in *ASMase*$^{+/+}$ mice at various time points after Gal/LPS treatment with or without SAM therapy.

cosphingolipid synthesis, decreasing the stimulation of GD3 and GM1 levels by TNF-α (325% ± 56% or 298% ± 76% vs. 8% ± 5% or 3% ± 4% for GD3 and GM1 in the absence or presence of D-*threo*-PDMP, respectively; P < 0.05). As expected, D-*threo*-PDMP enhanced TNF-α–generated ceramide levels (2.3 ± 0.3–fold; P < 0.05). However, under these conditions the downregulating effect of TNF-α on MAT1A expression was not affected by D-*threo*-PDMP (Figure 1A). Similar findings were observed using *N*-butyldeoxynojirimycin, another GCS inhibitor (not shown). Thus, these findings show the ability of ceramide generated specifically from hASMase to downregulate the expression of MAT1A and exclude the possibility of a role for glycosphingolipids in this effect.

Abolishment of intracellular vesicle acidification prevents downregulation of MAT1A mRNA by hASMase. We have previously shown that exogenous hASMase enters hepatocytes by endocytosis being delivered to intracellular acidic compartments (37). To assess whether hASMase requires acidic vesicles for its effect on MAT1A expression, we next determined the effect of lysosomotropic agents that abolish acidification of intracellular vesicles. As shown (Figure 2), bafilomycin A1, an inhibitor of the H^+-ATPase pump responsible for acidifying lysosomes and late endosomes (45), and chloroquine, known to disrupt acidic compartments (46), each prevented the downregulation of MAT1A induced by hASMase (Figure 2). Moreover, M 6-P, which blocks the delivery to endosomes/lysosomes of enzymes via the M 6-P receptor (47), abolished the reduction in MAT1A mRNA by hASMase (Figure 2). A similar effect for bafilomycin A1 and chloroquine was observed in the TNF-α–mediated downregulation of MAT1A mRNA levels (not shown). Thus, these findings indicate that the internalization of hASMase into acidic vesicles is required for the downregulation of MAT1A mRNA.

Structural requirement of ceramide in the downregulation of MAT1A. To assess the structural requirement of ceramide, we tested the role of sphingolipid analogs on MAT1A expression. As seen, membrane-permeant ceramide C2, as well as glycosphingolipids GD3, GM3, lactosylceramide, and glucosylceramide, reduced MAT1A mRNA levels to a similar extent while increasing those of MAT2A (Figure 3). Similar findings were observed for MAT1A regulation using the natural ceramide C16 (not shown). In contrast, incubation of cells with sphingomyelin, sphingosine, or dihydroceramide C2 did not change the relative levels of MAT1A or of MAT2A mRNA. In addition, incubation of cells with lyso-lactosylceramide (Matreya) did not affect the level of MAT1A or MAT2A mRNA (not shown). Thus, taking into account that carbohydrates are present only in glycosphingolipids but not in sphingolipids and that the *N*-fatty acyl-sphingosine moiety and the *trans*-4,5 double bond are structural features common to both lipid classes, it appears that the carbohydrate groups are not required for the regulation of MAT1A expression.

TNF-α fails to downregulate MAT1A in hepatocytes from ASMase-deficient mice. To assess the specific role of ASMase in the regulation of MAT1A by TNF-α, we used hepatocytes from *ASMase*$^{-/-}$ mice, as early signaling events in response to TNF-α are preserved in ASMase knockout mice (21). Compared with those in *ASMase*$^{+/+}$ cells, the levels of MAT1A mRNA in hepatocytes lacking the *ASMase* gene were unaffected upon exposure to TNF-α (Figure 4, A and B). However,

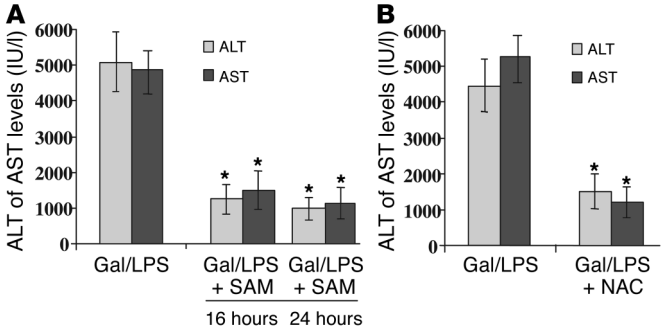

Figure 8
Protection against liver failure by chronic SAM treatment or antioxidants. (**A**) *ASMase*$^{+/+}$ mice treated with Gal/LPS were administered SAM for 16 or 24 hours, and liver damage was assessed by serum transaminase analyses. Data are the mean ± SD of ten individual experiments. *P = 0.05 versus Gal/LPS. (**B**) Alternatively, *ASMase*$^{+/+}$ mice were treated with NAC instead of SAM to analyze its effect on liver injury induced by Gal/LPS, as assessed by serum transaminases. Data are the mean ± SD of four individual experiments. *P = 0.05 versus Gal/LPS.

despite the unresponsiveness of *ASMase*$^{-/-}$ hepatocytes to TNF-α exposure, the addition of exogenous hASMase markedly decreased the levels of MAT1A mRNA while increasing those of MAT2A (Figure 4B). This effect was specific for ceramide derived from hASMase, as incubation of cells with exogenous bNSMase did not affect MAT1A or MAT2A mRNA content (Figure 4). These results show that the repressive effect of TNF-α on MAT1A expression is mediated through the generation of ceramide from ASMase.

Hepatic SAM levels in ASMase$^{-/-}$ *mice during lethal hepatitis*. To address whether the contribution of ASMase to TNF-α–induced liver injury is through MAT1A downregulation and subsequent SAM decrease, we examined the changes over time of hepatic SAM produced by Gal and TNF-α or LPS in a well-established model of lethal hepatitis (41, 42). In *ASMase*$^{+/+}$ mice (n = 25), Gal/TNF caused a time-dependent decrease of the hepatocellular SAM levels before the occurrence of liver damage, as monitored by the rise in ALT in serum (Figure 5A). Histological examination of liver samples from Gal/TNF- or Gal/LPS-treated mice indicated extensive hemorrhagic lesions with clusters of damaged cells (Figure 5B). TUNEL assay showed the presence of apoptotic hepatocytes in liver specimens from Gal/LPS-treated wild-type mice (Figure 6A). In contrast, the hepatic levels of SAM in *ASMase*$^{-/-}$ mice treated with Gal/TNF remained significantly higher than those in wild-type mice, and this outcome was accompanied by minimal liver damage, as monitored by serum transaminases (Figure 5A), liver histology (Figure 5B), and TUNEL assay (Figure 6A). Northern blot analyses indicated a decrease in MAT1A mRNA levels in *ASMase*$^{+/+}$ mice by 3 hours after Gal/TNF treatment (not shown). The hepatocellular levels of SAM in the ASMase knockout mice after Gal/TNF treatment were similar to those in *ASMase*$^{+/+}$ mice treated with Gal alone (63 ± 5 nmol/g liver and 53 ± 6 nmol/g liver 3 hours and 6 hours after, respectively). As this model of liver injury is caspase dependent, we examined the activation of caspases 8 and 3 in liver samples after Gal/TNF administration by a fluorescence assay using appropriate substrates and by immunoblot. Although each approach showed activation of caspases 3 and 8 by Gal/TNF in hepatocytes from wild-type mice (Figures 5C and 6, B and C), interestingly, caspase activation was much lower in *ASMase*$^{-/-}$ mice treated with Gal/TNF than in *ASMase*$^{+/+}$ mice (Figures 5C and 6, B and C), suggesting that ASMase is necessary for optimal caspase activation in this model. Furthermore, as hepatic SAM regulates GSH homeostasis, which in turn can modulate caspase activation (48, 49), we next determined the time course of hepatic GSH levels in this model of hepatocellular cell death. As seen, hepatic GSH levels decreased in *ASMase*$^{+/+}$ mice over time, lagging behind the reduction in SAM content in *ASMase*$^{+/+}$ mice but not in *ASMase*$^{-/-}$ mice (Figure 5, A and D). Similar results were observed with Gal/LPS (not shown). Finally, the levels of mitochondrial GSH, an essential pool of GSH in the control of mitochondrial function and cell death (21, 40), were reduced to 51 ± 7% of control levels in *ASMase*$^{+/+}$ mice (Figure 5E).

Lethal liver failure in ASMase$^{+/+}$ *mice is prevented by SAM administration*. Because the fall in SAM levels was a primary event in this model of liver failure, we next examined the therapeutic role of SAM in *ASMase*$^{+/+}$ mice. Initial experiments indicated that a single intraperitoneal injection of 10 mg/kg of SAM, a dose previously used in experimental models of liver injury and fibrogenesis (33, 50), before Gal/TNF or Gal/LPS administration was ineffective in preserving hepatic SAM levels and in preventing liver damage (not shown). However, continuous SAM treatment, hourly after Gal/LPS exposure, prevented liver injury through restoration of hepatic SAM (Figure 7, A–C). Furthermore, SAM treatment decreased caspase activation, as assessed by immunoblot (Figure 6, B and C) or stimulated fluorescence (Figure 7D), and these effects were accompanied by restoration of intracellular GSH stores in cytosol (Figure 7E) and mitochondria (Figure 5E). Indeed, the specific contribution of GSH to the protective effect of SAM was further assessed by treatment of mice with BSO, an inhibitor of γ-GCS. Pretreatment of *ASMase*$^{+/+}$ mice with BSO after Gal/LPS administration abolished the protective effect of SAM treatment (Figure 7, A and B). BSO treatment, however, did not affect the levels of SAM but prevented the recovery of GSH (not shown). In addition, to ensure that the protective effect of SAM was not due to reduced TNF-α secretion caused by LPS, we monitored plasma TNF-α levels over time. As seen, the time course of TNF-α appearance in plasma was similar in Gal/LPS-treated mice with or without SAM therapy (Figure 7F). Moreover, we checked the safety of chronic SAM therapy in Gal/LPS-treated mice. As seen, sustained administration of SAM was safe and devoid of side effects, as mice were protected from Gal/LPS-induced liver damage (Figure 8A). In addition, NAC, an antioxidant, reduced the liver injury caused by Gal/LPS (Figure 8B).

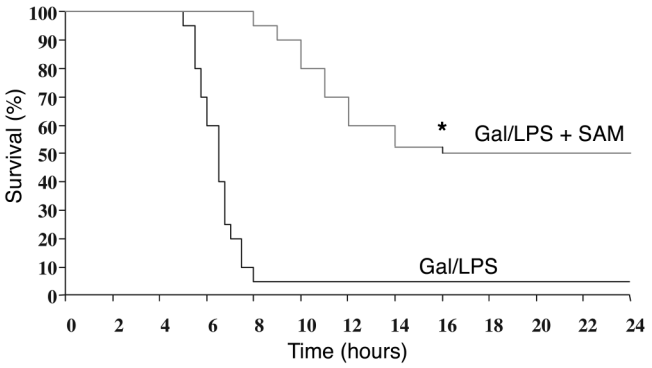

Figure 9
Effect of SAM therapy on survival of mice treated with Gal/LPS. *ASMase*$^{+/+}$ mice (n = 30) were treated with Gal/LPS; half were treated with SAM (Gal/LPS + SAM) and the other half were treated with saline (Gal/LPS) every hour for 8 hours. The percentage of dying mice was plotted as a function of time after induction of hepatitis. *P < 0.05 vs. Gal/LPS group.

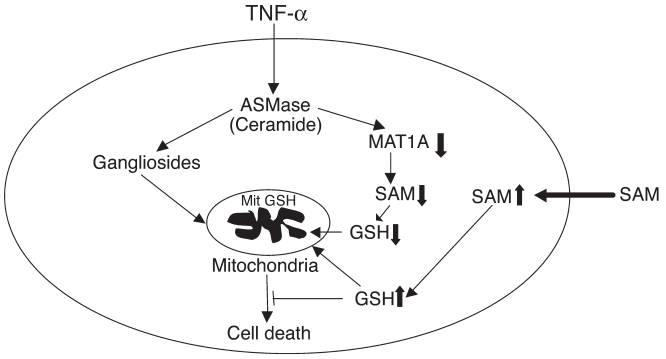

Figure 10
Scheme depicting the mechanisms used by ASMase in mediating the cytotoxic effects of TNF-α. Our present findings illustrate the consequences of the downregulation of MAT1A by ASMase resulting in GSH depletion, particularly in the mitochondria, subsequent to the decrease in SAM levels. Although this mechanism leaves hepatocytes unprotected, glycosphingolipids, especially GD3, synthesized from the pool of ceramide generated by ASMase activation, increase and traffic to the mitochondria, initiating the apoptosome activation responsible for hepatocellular apoptosis and liver failure. Both processes promote the damaging effects induced by TNF-α. SAM treatment would replenish GSH stores, including those in mitochondria (Mit), producing favorable conditions in which hepatocytes withstand the effects of TNF-α.

Finally, the protective role of SAM "translated" to an improved survival rate (Figure 9). As seen, mice (n = 15) treated with SAM were significantly protected from lethality, compared with the control group treated with saline. Surviving mice were still alive for at least 5 days after the Gal/LPS treatment. Treatment of mice with SAM for 24 hours resulted in a similar survival rate (not shown). Similar results in terms of survival were observed in mice treated with Gal/TNF instead of LPS. In addition, 80–90% of *ASMase*$^{-/-}$ mice survived at least 5 days after Gal/TNF treatment.

Discussion

The present study reveals a novel mechanism of action of ASMase whereby this signaling enzyme promotes TNF-α–induced hepatocellular damage by decreasing the expression of MAT1A. Our first approach was the use of exogenous hASMase. Certain structural features of this enzyme have been characterized in comparison with those of recombinant human ASMase (51). Those studies demonstrated that recombinant human ASMase and the native protein purified from human placenta showed a similar glycosylation pattern and the presence of a critical disulfide bond in the sphingolipid activator N-terminal domain. In addition, prior studies demonstrated that hASMase enters cells including hepatocytes via M 6-P receptor–mediated endocytosis and is delivered into acidic compartments (37, 47, 52). Consistent with the pH optima of hASMase, we verified that agents that block intracellular vesicle acidification abolished the effect of hASMase on MAT1A expression. In addition, the action of hASMase on MAT1A expression was prevented by an excess of M 6-P, which would be expected to compete with hASMase for endocytosis without dissipating the pH gradient of acidic intracellular compartments. Thus, based on these findings it appears that endocytosis of hASMase and its delivery into acidic vesicles where the enzyme becomes active are required for the downregulation of MAT1A expression. However, the precise intracellular site where hASMase becomes activated remains to be identified. In addition to this approach, we also used hepatocytes deficient in *ASMase*$^{-/-}$. The data we obtained show the resistance of hepatocytes from ASMase knockout mice to TNF-α–induced downregulation of MAT1A. However, the levels of MAT1A mRNA were reduced by hASMase, indicating that the response of hepatocytes from ASMase knockout mice to TNF-α in the regulation of MAT1A is dependent on the presence of ASMase.

An important implication from these results is the divergent functions of NSMase versus ASMase in the regulation of MAT1A expression. Not only did bNSMase, a Mg^{2+}-dependent exogenous SMase at neutral pH, characterized previously (8, 9, 37), fail to affect the expression of MAT1A, but also, more importantly, the activation of NSMase by TNF-α remains intact in hepatocytes from ASMase knockout mice (21) and yet in *ASMase*$^{-/-}$ hepatocytes, TNF-α failed to downregulate MAT1A. Thus, our findings clearly indicate that the ceramide pool signaling the downregulation of MAT1A originates from an acidic intracellular compartment, whereas the ceramide pool derived from NSMase is inactive, illustrating that the role of ceramide in cell signaling depends on the specific SMase activated. This outcome regarding the effect of ASMase on gene regulation contrasts with previous reports discarding a role for ceramide produced in lysosomes in apoptosis signaling. For instance, stress-induced apoptosis was observed in Epstein-Barr virus–transformed B lymphocytes from control individuals as well as from patients affected with Niemann-Pick disease, an autosomal recessive condition characterized by deficient ASMase in lysosomes (14). In contrast, DeMaria et al. (52), who also used Niemann-Pick lymphoblast lines, concluded that ASMase was required for Fas-mediated apoptosis. On the other hand, hepatocytes deficient in ASMase have been shown to be resistant to ionizing radiation–, Fas- or TNF-α–mediated cell death (15, 19–21). Furthermore, consistent with our findings regarding MAT1A regulation, Monney et al. (53) reported that agents that alkalinize acidic vesicles attenuate TNF-α–induced apoptosis in U937 human monocytes and L292 mouse fibroblasts. Thus, it appears that the role of individual SMases in signaling pathways (apoptosis or gene regulation) depends on several conditions, such as the stimuli used and type of cell studied. Hence, taken collectively, our data establish that MAT1A is selectively downregulated by ceramide generated from the activation of ASMase in acidic intracellular compartments, which mediates the effects observed with TNF-α.

Of note, we would like to emphasize that the downregulating effect of TNF-α or hASMase on MAT1A mRNA levels was observed despite the presence of exogenous SAM, which stimulates the transcription of *MAT1A* (44). Thus, in further examining the putative mechanism involved in the downregulation of MAT1A by ASMase, we determined the stability of MAT1A mRNA in the presence of actinomycin D. Our data show that the presence of hASMase shortened the half-life of MATA1 mRNA from 5.4 ± 0.3 hours to 3.3 ± 0.2 hours (P = 0.005). In an attempt to characterize this process further, we observed that cycloheximide pretreatment abolished the effect of hASMase on MAT1A mRNA decay, suggesting the involvement of specific proteins. Thus, although at present we do not understand the mechanism involved in the posttranscriptional decay of MAT1A mRNA by ASMase, an important pathway in the control of mRNA includes the recruitment of the exosome by AU-binding proteins to affect 3′-to-5′ mRNA degradation (54). Although clearly more work will be required to fully characterize this novel mechanism in the regulation of MAT1A expression by ASMase-induced ceramide generation, including the identification of the specific proteins involved and the role of the AU site in the 3′ untranslated region of *MAT1A*, similar effects on the modulation of mRNA stability have been described recently for

cell-permeable ceramides in other cell types. For instance, in Jurkat cells, ceramide C2 shortened the half-life of Bcl-2 mRNA through a conserved AU-rich element in the 3′ untranslated region of Bcl-2 mRNA (55). In addition, other remaining questions include how ceramide recruits or activates this regulated pathway (54). Whether ceramide generated within acidic vesicles undergoes a transbilayer movement similar to what has been recently reported for bNSMase (56) in erythrocyte ghosts remains to be established. In hepatocytes we have shown that the ceramide pool generated from bNSMase must undergo a "flip-flop" movement across the bilayer to signal the transcriptional regulation of genes such as γ-GCS (37).

To examine the in vivo consequences of the downregulation of MAT1A by ASMase, we analyzed the regulation of hepatic SAM during the progression of liver failure in a model of lethal hepatitis. This approach revealed that the depletion of hepatocellular SAM levels precedes the activation of caspases induced by TNF-α, resulting in liver damage and lethality. The outcome of *ASMase*$^{-/-}$ mice challenged with Gal/TNF was similar to that of *ASMase*$^{+/+}$ mice treated with Gal alone. In both cases, the mild decrease in hepatic SAM reflects the effect of Gal, a hepatotoxin that blocks transcription in hepatocytes. MAT I/III is sensitive to oxidative stress due to the targeting of a critical cysteine residue (30, 32). Hence the downregulation of MAT1A and the inactivation of MAT I/III accelerate the depletion of SAM by TNF-α in *ASMase*$^{+/+}$ mice, initiating a cascade of events that culminate in the death of mice. As shown by TUNEL assay, the fulminant outcome of this model reflects a prominent hepatocellular apoptosis. In comparing caspase activation in *ASMase*$^{-/-}$ versus *ASMase*$^{+/+}$ mice, we unexpectedly observed a defective activation of caspase 8 by TNF-α in ASMase knockout mice. Previous findings reported the involvement of upstream caspases, such as caspase 8, in the activation of ASMase (57–59); however, our data indicate that ASMase is needed for optimal caspase 8 activation by TNF-α (Figure 5C) and suggest an inverse hierarchical ordering in caspase 8/ASMase activation, as reported for Fas (58, 59). This effect seems to be dependent on SAM through replenishment of GSH levels, as SAM therapy attenuated caspase 8 activation in *ASMase*$^{+/+}$ mice (Figure 7D). Furthermore, our findings also indicate the regulation of caspase 3 by ASMase. In the absence of ASMase, we observed a lowered activation of caspase 3 by TNF-α (Figures 5C and 6B), and this ASMase-independent caspase 3 activation may be due to the participation of other signaling proteins, such as cathepsin B (5). In addition, SAM seems to regulate caspase 3 activation. This outcome may reflect the ability of SAM to regulate the mitochondrial commitment to cell death (60, 61). Depletion of SAM in the livers of *MAT1A*$^{-/-}$ knockout mice has been shown to modulate mitochondrial integrity through regulation of the expression of prohibitin, a protein encoded in the nucleus that participates in the functional organization of mitochondria (60). However, in addition to this potential mechanism, it is likely that the protective effect of SAM in lethal hepatitis is dependent on the replenishment of GSH levels, particularly in mitochondria (39, 62), as BSO pretreatment abrogated the therapeutic role of SAM. Indeed, mitochondrial GSH has been shown to play an essential role in the survival of hepatocytes in the face of TNF-α–mediated cell death (21, 37, 40, 62).

The present study complements recent observations on the mechanisms of TNF-α–induced hepatocellular damage (21) (Figure 10). Through MAT1A downregulation and subsequent SAM decrease, mitochondrial GSH levels become limited, leaving hepatocytes unprotected from death signals generated by TNF-α–induced ASMase activation, such as GD3 (21). As GD3 can target mitochondria (63), the consequences of this interaction, which leads to apoptosome assembly and caspase 3 activation, depend largely on the levels of mitochondrial GSH (21, 43, 63). Thus, the combination of mitochondrial GSH depletion and the trafficking of GD3 to mitochondria mediates the hepatocellular damage of TNF-α. An implication of the current and previous findings (21) is that in addition to the therapeutic effect of SAM, interference with ASMase signaling may be beneficial, as it would spare SAM/GSH levels and avoid the production of harmful lipids such as GD3. The effects of ASMase inhibitors in vivo on liver function and protection against liver failure remain to be established, however.

Taken together, our findings characterize a novel function of ASMase in the cytotoxicity of TNF-α. Given that TNF-α is essential in several forms of liver damage, such as alcohol-induced liver injury (31, 40) and lethal hepatitis (41, 42), our findings may be of therapeutic relevance for the prevention of fulminant liver failure and the treatment of liver diseases through replenishment of SAM and subsequent restoration of mitochondrial GSH.

Acknowledgments

We want to express our gratitude to R. Kolesnick and E. Gulbins for the gift of ASMase knockout mice, and M. Pajares for anti–MAT I/III. The work presented was supported in part by the Research Center for Liver and Pancreatic Diseases, P50 AA 11999; and grant 1R21 AA014135-01, funded by the US National Institute on Alcohol Abuse and Alcoholism; Plan Nacional de I+D grants SAF01-2118, SAF2002-3564, and SAF2003-04974; and Red Temática de Investigación Cooperativa G03/015 and Red de Centros C03/02, supported by Instituto de Salud Carlos III. We want to thank Susana Nuñez for expert technical assistance and genotyping of *ASMase*$^{-/-}$ mice. M. Marí and A. Morales are Ramón y Cajal investigators.

Received for publication August 20, 2003, and accepted in revised form January 13, 2004.

Address correspondence to: José C. Fernández-Checa, Liver Unit, Institut de Malalties Digestives, Hospital Clínic i Provincial, C/ Villarroel 170, 08036-Barcelona, Spain. Phone: 34-93-2275709; Fax: 34-93-451 5272; E-mail: checa229@yahoo.com.

1. Bird, G.L.A., Sheron, N., Goka, J., Alexander, G.J., and Williams, R.S. 1990. Increased plasma tumor necrosis factor in severe alcoholic hepatitis. *Ann. Intern. Med.* **112**:917–920.
2. Muto, Y., et al. 1988. Enhanced tumour necrosis factor and interleukin-1 in fulminant hepatic failure. *Lancet.* **2**:72–74.
3. Gonzalez-Amaro, R., et al. 1994. Induction of tumor necrosis factor production by human hepatocytes in chronic viral hepatitis. *J. Exp. Med.* **179**:841–848.
4. Zhang, R., et al. 2003. AIP1 mediates TNF-α-induced ASK1 activation by facilitating dissociation of ASK1 from its inhibitor 14-3-3. *J. Clin. Invest.* **111**:1933–1943. doi:10.1172/JCI200317790.
5. Guicciardi, M.E., et al. 2000. Cathepsin B contributes to TNF-α–mediated hepatocyte apoptosis by promoting mitochondrial release of cytochrome *c*. *J. Clin. Invest.* **106**:1127–1137.
6. Kolesnick, R. 2002. The therapeutic potential of modulating the ceramide/sphingomyelin pathway. *J. Clin. Invest.* **110**:3–8. doi:10.1172/JCI200216127.
7. Hannun, Y.A., and Luberto, C. 2000. Ceramide in the eukaryotic stress response. *Trends Cell Biol.* **10**:73–80.
8. Kolesnick, R.N., and Kronke, M. 1998. Regulation of ceramide production and apoptosis. *Annu. Rev. Physiol.* **60**:643–665.
9. Wiegman, K., Schutze, S., Machleidt, T., Witte, D., and Kronke, M. 1994. Functional dichotomy of neutral and acid sphingomyelinase in tumor necrosis factor signaling. *Cell.* **78**:1005–1015.
10. Hannun, Y.A., Luberto, C., and Argraves, K.M. 2001. Enzymes of sphingolipid metabolism: from modular to integrative signaling. *Biochemistry.* **40**:4893–4903.
11. Spiegel, S., and Merrill, A.H., Jr. 1996. Sphingolipid

metabolism and growth regulation. *FASEB J.* **10**:1388–1397.
12. Liu, P., and Anderson, G.G.W. 1995. Compartmentalized production of ceramide at the cell surface. *J. Biol. Chem.* **270**:27179–27185.
13. Schissel, S.L., Schuchman, E.H., Williams, K.J., and Tabas, I. 1996. Zn^{2+}-stimulated sphingomyelinase is secreted by many cells and is a product of the acid sphingomyelinase gene. *J. Biol. Chem.* **271**:18431–18436.
14. Bezombes, C., et al. 2001. Lysosomal sphingomyelinase is not solicited for apoptotic signaling. *FASEB J.* **15**:297–299.
15. Lozano, J., et al. 2001. Cell autonomous apoptosis defects in acid sphingomyelinase knockout fibroblasts. *J. Biol. Chem.* **276**:442–448.
16. Grullich, C., Sullards, M.C., Fuks, Z., Merrill, A.H., Jr., and Kolesnick, R. 2000. CD95 (Fas/APO-1) signals ceramide generation independent of the effector stage of apoptosis. *J. Biol. Chem.* **275**:8650–8656.
17. Morita, Y., et al. 2000. Oocyte apoptosis is suppressed by disruption of the acid sphingomyelinase gene or by sphingosine-1-phosphate therapy. *Nat. Med.* **6**:1109–1114.
18. Segui, B., et al. 2001. Involvement of FAN in TNF-induced apoptosis. *J. Clin. Invest.* **108**:143–151. doi:10.1172/JCI200111498.
19. Lin, T., et al. 2000. Role of acidic sphingomyelinase in Fas/CD95-mediated cell death. *J. Biol. Chem.* **275**:8657–8663.
20. Paris, F., et al. 2001. Natural ceramide reverses Fas resistance of acid sphingomyelinase (–/–) hepatocytes. *J. Biol. Chem.* **276**:8297–8305.
21. García-Ruiz, C., et al. 2003. Defective TNF-α-mediated hepatocellular apoptosis and liver damage in acidic sphingomyelinase knockout mice. *J. Clin. Invest.* **111**:197–208. doi:10.1172/JCI200316010.
22. Finkelstein, J.D. 1990. Methionine metabolism in mammals. *J. Nutr. Biochem.* **1**:228–236.
23. Mato, J.M., Alvarez, L., Ortiz, P., and Pajares, M.A. 1997. S-adenosylmethionine synthesis: molecular mechanisms and clinical implications. *Pharmacol. Ther.* **73**:265–280.
24. Avila, M.A., et al. 2002. S-adenosylmethionine revisited: its essential role in the regulation of liver function. *Alcohol.* **27**:163–167.
25. Farooqui, J.Z., Lee, H.W., Kim, S., and Paik, W.K. 1983. Studies on compartmentation of S-adenosyl-L-methionine in saccharomyces cerevisiae and in isolated rat hepatocytes. *Biochim. Biophys. Acta.* **757**:342–351.
26. Trunpower, B.L., Houser, R.M., and Olson, R.E. 1974. Studies on ubiquinone. Demonstration of the total biosynthesis of ubiquinone in rat liver mitochondria. *J. Biol. Chem.* **249**:3041–3048.
27. Cabrero, C., Puerta, J., and Alemany, S. 1987. Purification and comparison of two forms of S-adenosyl-L-methionine synthetase from rat liver. *Eur. J. Biochem.* **170**:299–304.
28. Lombardini, J.B., Chou, T.C., and Talalay, P. 1973. Regulatory properties of adenosine triphosphate-L-methionine S-adenosyltransferase of rat liver. *Biochem. J.* **135**:43–57.
29. LeGros, H.L., Jr., Halim, A.B., Geller, A.M., and Kotb, M. 2000. Cloning, expression, and functional characterization of the β regulatory subunit of human methionine adenosyltransferase (MAT II). *J. Biol. Chem.* **275**:2359–2366.
30. Mato, J.M., Corrales, F.J., Ortiz, P., and Avila, M.A. 2001. *S-adenosylmethionine in the treatment of liver disease.* C.S. Lieber, editor. UTET periodici. Milano, Italy. 1–21.
31. Mato, J.M., et al. 1999. S-adenosylmethionine in alcoholic liver cirrhosis: a randomized, placebo-controlled, double-blind, multicenter clinical trial. *J. Hepatol.* **30**:1081–1089.
32. Martin Duce, A., Ortiz, P., Cabrero, C., and Mato, J.M. 1988. S-adenosyl-L-methionine synthetase and phospholipid methyltransferase are inhibited in human cirrhosis. *Hepatology.* **8**:65–68.
33. Corrales, F., et al. 1992. S-adenosylmethionine treatment prevents carbon tetrachloride-induced S-adenosyl-L-methionine synthetase inactivation and attenuates liver injury. *Hepatology.* **16**:1022–1027.
34. Lu, S.C., et al. 2001. Methionine adenosyltransferase 1A knockout mice are predisposed to liver injury and exhibit increased expression of genes involved in proliferation. *Proc. Natl. Acad. Sci. U. S. A.* **98**:5560–5565.
35. Martínez-Chantar, M.L., et al. 2002. Spontaneous oxidative stress and liver tumors in mice lacking methionine adenosyltransferase 1A. *FASEB J.* **16**:1292–1294.
36. Chen, J., Nikolova-Karakashian, M., Merrill, A.H., Jr., and Morgan, E.T. 1995. Regulation of cytochrome P450 2C11 (CYP2C11) gene expression by interleukin-1, sphingomyelin hydrolysis, and ceramides in rat hepatocytes. *J. Biol. Chem.* **270**:25233–25238.
37. García-Ruiz, C., et al. 2000. Human placenta sphingomyelinase, an exogenous acidic pH-optimum sphingomyelinase, induces oxidative stress, glutathione depletion, and apoptosis in rat hepatocytes. *Hepatology.* **32**:56–65.
38. Frago, L.M., Pañeda, C., Fabregat, I., and Varela-Nieto, I. 2001. Short-chain ceramide regulates hepatic methionine adenosyltransferase expression. *J. Hepatol.* **34**:192–201.
39. Mingorance, J., Alvarez, L., Sánchez-Góngora, E., Mato, J.M., and Pajares, M.A. 1996. Site-directed mutagenesis of rat liver S-adenosylmethionine synthetase. Identification of a cysteine residue critical for the oligomeric state. *Biochem. J.* **315**:761–766.
40. Colell, A., et al. 1998. Selective glutathione depletion of mitochondria sensitizes hepatocytes to tumor necrosis factor. *Gastroenterology.* **115**:1541–1551.
41. Lehmann, V., Freudenberg, M.A., and Galanos, C. 1987. Lethal toxicity of lipopolysaccharide and tumor necrosis factor in normal and D-galactosamine-treated mice. *J. Exp. Med.* **165**:657–663.
42. Wielockx, B., et al. 2001. Inhibition of matrix metalloproteinases blocks lethal hepatitis and apoptosis induced by tumor necrosis factor and allows safe antitumor therapy. *Nat. Med.* **7**:1202–1208.
43. García-Ruiz, A., Colell, A., Paris, R., and Fernández-Checa, J.C. 2000. Direct interaction of GD3 ganglioside with mitochondria generates reactive oxygen species followed by mitochondrial permeability transition, cytochrome c release and caspase activation. *FASEB J.* **14**:847–858.
44. García-Trevijano, E.R., et al. 2000. S-adenosylmethionine regulates MAT1A and MAT2A gene expression in cultured rat hepatocytes: a new role for S-adenosylmethionine in the maintenance of the differentiated status of the liver. *FASEB J.* **14**:2511–2518.
45. Bowman, E.J., Siebers, A., and Altendorf, K. 1988. Bafilomycins: a class of inhibitors of membrane ATPases from microorganisms, animal cells and plant cells. *Proc. Natl. Acad. Sci. U. S. A.* **85**:7972–7976.
46. Hurwitz, S.J., Terashima, M., Mizunuma, N., and Slapak, C.A. 1997. Vesicular antracycline accumulation in doxorubicin-selected U-937 cells: participation of lysososmes. *Blood.* **89**:3745–3754.
47. Dahms, N.M., Lobel, P., and Kornfeld, S. 1989. Mannose 6-phosphate receptors and lysosomal enzyme targeting. *J. Biol. Chem.* **264**:12115–12118.
48. Hentze, H., et al. 2002. Glutathione dependence of caspase-8 activation at the death-inducing signaling complex. *J. Biol. Chem.* **277**:5588–5595.
49. Chiba, T., Takahashi, S., Sato, N., Ishii, S., and Kikuchi, F. 1996. Fas-mediated apoptosis is modulated by intracellular glutathione in human T cells. *Eur. J. Immnunol.* **26**:1164–1169.
50. Gasso, M., et al. 1996. Effects of S-adenosylmethionine on lipid peroxidation and liver fibrogenesis in carbon tetrachloride-induced cirrhosis. *J. Hepatol.* **25**:200–205.
51. Lansmann, S., et al. 2003. Human acid sphingomyelinase. Assignment of the disulfide bond pattern. *Eur. J. Biochem.* **270**:1076–1088.
52. De Maria, R., Rippo, M.R., Schuchman, E.H., and Testi, R. 1998. Acidic sphingomyelinase is necessary for Fas-mediated GD3 ganglioside accumulation and efficient apoptosis of lymphoid cells. *J. Exp. Med.* **187**:897–902.
53. Monney, L., et al. 1998. Role of an acidic compartment in tumor necrosis factor-α-induced production of ceramide, activation of caspase 3 and apoptosis. *Eur. J. Biochem.* **251**:295–303.
54. Chen, C.Y., et al. 2001. AU binding proteins recruit the exosome to degrade ARE-containing mRNAs. *Cell.* **107**:451–464.
55. Schiavone, N., et al. 2000. A conserved AU-rich element in the 3′ untranslated region of bcl-2 mRNA is endowed with a destabilizing function that is involved in bcl-2 down-regulation during apoptosis. *FASEB J.* **14**:174–184.
56. Contreras, F.X., Villar, A.V., Alonso, A., Kolesnick, R.N., and Goñi, F.M. 2003. Sphingomyelinase activity causes transbilayer lipid translocation in model and cell membranes. *J. Biol. Chem.* **278**:37169–37174.
57. Schwander, R., Wiegmann, K., Bernardo, K., Kreder, D., and Kronke, M. 1998. TNF receptor death domain-associated proteins TRADD and FADD signal activation of acid sphingomyelinase. *J. Biol. Chem.* **273**:5916–5922.
58. Brenner, B., et al. 1998. Fas/CD95/Apo-I activates the acidic sphingomyelinase via caspases. *Cell Death Differ.* **5**:29–37.
59. Sawada, M., et al. 2002. Acid sphingomyelinase activation requires caspase 8 but not p53 nor reactive oxygen species during Fas-induced apoptosis in human glioma cells. *Exp. Cell Res.* **273**:157–168.
60. Santamaria, E., et al. 2003. Functional proteomics of nonalcoholic steatohepatitis: mitochondrial proteins as targets of S-adenosylmethionine. *Proc. Natl. Acad. Sci. U. S. A.* **100**:3065–3070.
61. Ansorena, E., et al. 2002. S-adenosylmethionine and methylthioadenosine are antiapoptotic in cultured rat hepatocytes but proapoptotic in human hepatoma cells. *Hepatology.* **35**:274–280.
62. García-Ruiz, C., et al. 1995. Feeding S-adenosyl-L-methionine attenuates both ethanol-induced depletion of mitochondrial glutathione and mitochondrial dysfunction in periportal and perivenous rat hepatocytes. *Hepatology.* **21**:207–214.
63. García-Ruiz, C., et al. 2002. Trafficking of ganglioside GD3 to mitochondria by tumor necrosis factor-α. *J. Biol. Chem.* **277**:36443–36448.